

Supplementary Materials

In-situ Visualization of Reversible Diels-Alder Reactions with Self-Reporting Aggregation-Induced Emission Luminogens

Danning Hu,[†] Liucheng Mao,[†] Mengshi Wang,[†] Hongye Huang,[†] Renjian Hu,[†] Haijun Ma,[†]
Jinying Yuan,^{*‡} and Yen Wei^{*†§}

[†] Key Laboratory of Bioorganic Phosphorus Chemistry & Chemical Biology, Department of Chemistry, Tsinghua University, Beijing 100084, China.

[‡] Key Laboratory of Organic Optoelectronics & Molecular Engineering of Ministry of Education, Department of Chemistry, Tsinghua University, Beijing, 100084, China.

[§] Department of Chemistry, Center for Nanotechnology, Institute of Biomedical Technology, Chung Yuan Christian University, Taoyuan 32023, Taiwan, China.

* Corresponding author.

Email: weiyen@mail.tsinghua.edu.cn (Y.W.); yuanjy@mail.tsinghua.edu.cn (J.Y.)

Table of Contents

1. Materials and instrumentations

2. Syntheses and structural characterization (**Figure S1-S8**)

Figure S1-S6. ^1H and ^{13}C NMR spectra of TPEAM, TPEX, TPEMI, and TPE-DAs.

Figure S7. High-resolution mass spectra.

Figure S8. X-ray single-crystal diffraction structure analysis.

3. Optical characterization (**Figure S9-S11**)

Figure S9. UV-Vis absorption and emission properties of TPEMI and TPE-DAs.

Figure S10. Photos of 100 μM TPEMI and TPE-DAs in both good solvents and aqueous mixtures.

Figure S11. TEM and DLS results of the formation of the aggregates.

4. Intermolecular quenching effect in DA reaction mixture (**Figure S12-S15**)

Figure S12. Intermolecular quenching effect of TPEMI on TPE-B and TPE-C.

Figure S13. Intermolecular quenching effect of TPEMI in DMSO/water and THF/water mixtures.

Figure S14. Effect of the reactant, furan derivatives, on the fluorescence behavior.

Figure S15. Verification of quantitative equation.

5. Kinetics of reversible DA reaction (**Figure S16-S19**)

Figure S16. ^1H NMR spectral changes during TPE-A formation by the DA reaction.

Figure S17. Photos during TPE-A and TPE-B formation by the DA reactions.

Figure S18. Fluorescence kinetics of TPE-A to TPEMI conversion via RDA reactions.

Figure S19. ^1H NMR spectral changes during the RDA reactions.

6. Heterogeneous DA reaction and RDA reaction on solid state (**Figure S20-S23**)

Figure S20. Photos of the sample dots containing gradient amount of TPEMI and TPE-A under UV light.

Figure S21. Photos of heterogeneous DA reactions on silica plates.

Figure S22. Reversible fluorescent “ON-OFF” switching from TPEMI in solid state on a silica plate.

Figure S23. Photos of heterogeneous DA reactions and solid state RDA reactions.

1. Materials and instrumentations

All commercially available chemicals and reagents used as received without further purification. ^1H and ^{13}C NMR spectra were measured on a JEOL JNM-ECA400 (400 MHz) spectrometer (JEOL Co. Ltd., Tokyo, Japan) in $\text{DMSO-}d_6$ or $\text{Acetonitrile-}d_3$ using tetramethylsilane (TMS; $\delta = 0$ ppm) as the internal reference. The fluorescence spectra, quantum yield and lifetime were measured by a fluorescent photometer (SHIMADZU RF2000) at room temperature (25 °C). UV-Visible absorption spectra were recorded on a UV/Vis/NIR Perkin-Elmer lambda750 spectrometer (Waltham, MA, USA) using quartz cuvettes of 1 cm path length. The high resolution MS data were collected by a TIMS-TOF mass spectrometer (Bruker Daltonics, Bremen, Germany). X-ray crystal data of TPEMI were collected at 150 K by Rigaku Oxford diffraction system with a CCD detector and graphite-monochromated $\text{Cu } K\alpha$ radiation. Dynamic light scattering (DLS) analyses were performed at 25 °C on a Marven Zetasizer Nano ZS90 laser light scattering spectrometer with a 633 nm He-Ne laser at 90 ° angle. Morphology was observed by transmission electron microscopy (TEM) (HT7700, Hitachi, Japan).

2. Syntheses and structural characterization

Considering the accessibility and simplicity, commercially available TPE and its common derivatives are chosen as the core molecule with AIE character. To investigate the basic DA reaction process via fluorescence behaviors, in this work, no other functional group is designed onto TPEMI, and it can be obtained with a satisfactory yield by the Suzuki coupling reaction.

1-(4-Aminophenyl)-1,2,2-triphenylethene (TPEAM)

TPEAM was obtained by the Suzuki coupling reaction between triphenylvinyl bromide and 4-aminophenylboronic acid pinacol ester. In detail, a Schlenk tube was charged with triphenylvinyl bromide (2.682 g, 8 mmol), 4-aminophenylboronic acid pinacol ester (1.972 g, 9 mmol), potassium carbonate (2.211 g, 16 mmol), and tetrabutylammonium bromide (0.258 g, 0.8 mmol). Toluene (32 mL) and deionized water (10 mL) were then added. The mixture was thoroughly degassed before adding Tetrakis(triphenylphosphine)palladium catalyst (0.464 g, 0.4 mmol). The resulting mixture was stirred for 24 hours at 90 °C under an inert nitrogen atmosphere, then cooled to room temperature and extracted with ethyl acetate and washed by brine. Then the combined organic layer was filtered, concentrated and purified using column chromatography (silica gel, petroleum ether followed by PE/DCM 50:50, v/v). The pure product was a yellow solid with strong fluorescence (2.194 g, 79%).

^1H NMR (DMSO- d_6 , 400 MHz), δ (TMS, ppm): 7.17 - 6.96 (m, 13H), 6.92 (dd, J = 7.8, 1.4 Hz, 2H), 6.60 (d, J = 8.4 Hz, 2H), 6.30 (d, J = 8.4 Hz, 2H), 5.07 (s, 2H). ^{13}C NMR (DMSO- d_6 , 400 MHz), δ (TMS, ppm): 147.29, 144.20, 143.98, 143.95, 141.19, 137.86, 131.65, 130.91, 130.83, 130.75, 130.32, 127.77, 127.67, 127.57, 126.25, 126.00, 113.13. MS (ESI IT-TOF): m/z 348.1745 [$\text{M} + \text{H}^+$], calcd for $\text{C}_{26}\text{H}_{21}\text{N}$ [M]: 347.1674.

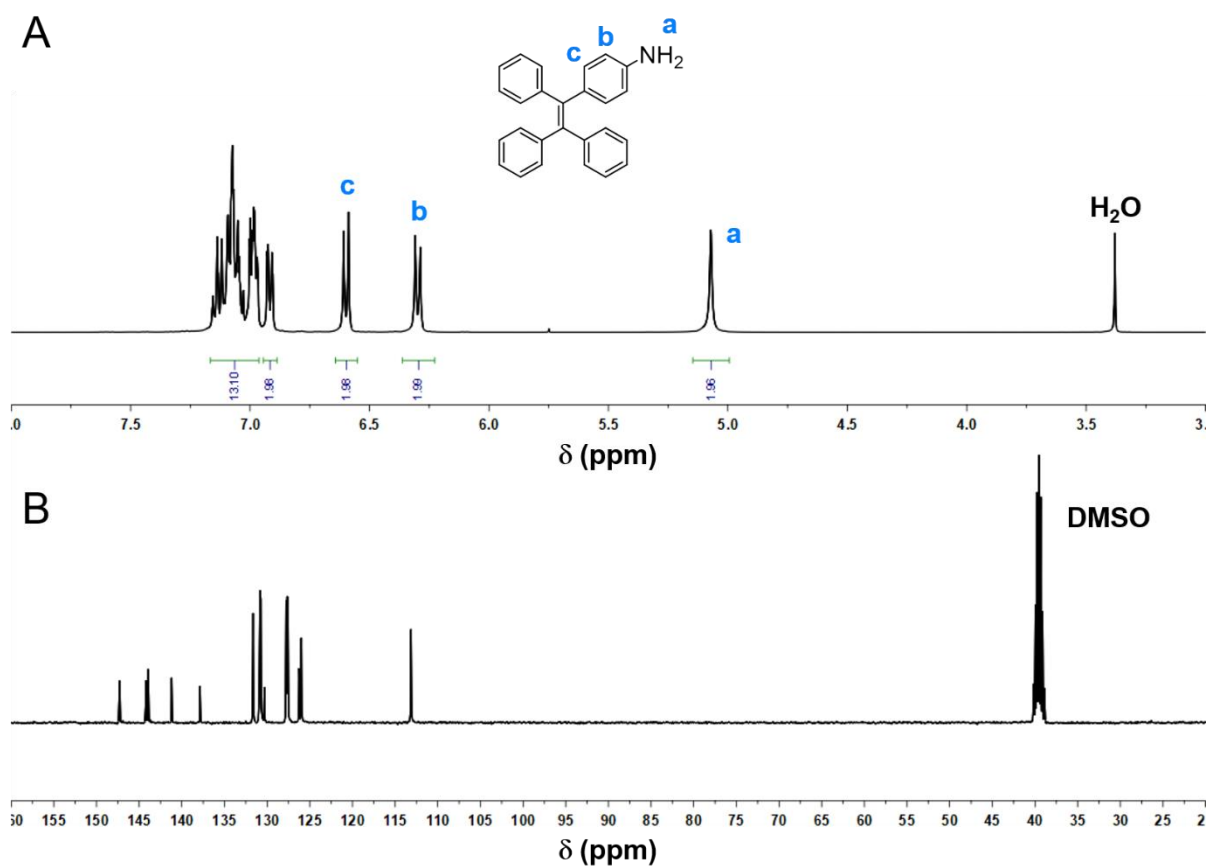


Figure S1. (A) ^1H and (B) ^{13}C NMR spectra of TPEAM in $\text{DMSO-}d_6$ with corresponding assignments.

1-(4-(1,2,2-triphenylvinyl)phenyl)- pyrrole-2,5-dione (TPEMI)

In a round bottom flask, a solution of TPEAM (0.695 g, 2 mmol) in 10 mL dichloromethane and maleic anhydride (0.98 g, 10 mmol) in 5 mL anhydrous diethyl ether was stirred at room temperature for 4 h. After washed with diethyl ether, a yellow solid of TPEX was obtained as an intermediate which directly underwent further reaction without purification. Anhydrous sodium acetate (1 g) and acetic anhydride (10 mL) were added to the flask and the mixture was stirred at 90 °C for 3 h. After cooling to room temperature, the solution was poured into cold deionized water. During this process, the TPEMI was precipitated as a yellow solid, which was isolated in 80% yield.

TPEX ^1H NMR (DMSO- d_6 , 400 MHz), δ (TMS, ppm): 13.08 (s, 1H), 10.34 (s, 1H), 7.37 (d, $J = 8.6$ Hz, 2H), 7.19 - 7.07 (m, 9H), 7.00 - 6.93 (m, 6H), 6.90 (d, $J = 8.5$ Hz, 2H), 6.41 (d, $J = 12.0$ Hz, 1H), 6.28 (d, $J = 12.0$ Hz, 1H). ^{13}C NMR (DMSO- d_6 , 100 MHz), δ (TMS, ppm): 167.36, 163.64, 143.79, 143.70, 140.83, 140.64, 139.21, 137.42, 132.13, 131.71, 131.25, 131.20, 130.90, 128.45, 128.34, 127.07, 119.32. MS (ESI IT-TOF): m/z 484.1311 [$\text{M} + \text{K}^+$], calcd for $\text{C}_{30}\text{H}_{23}\text{NO}_3$ [M]: 445.1678.

TPEMI ^1H NMR (DMSO- d_6 , 400 MHz), δ (TMS, ppm): 7.27 - 6.86 (m, 21H). ^1H NMR (ACETONITRILE- d_3 , 400 MHz), δ (TMS, ppm): 7.16 - 7.05 (m, 19H), 6.86 (s, 2H). ^{13}C NMR (DMSO- d_6 , 100 MHz), δ (TMS, ppm): 169.76, 143.04, 143.00, 142.96, 142.32, 141.11, 139.74, 134.61, 130.98, 130.66, 129.72, 127.94, 127.89, 127.79, 126.74, 126.63, 125.69. MS (ESI IT-TOF): m/z 450.1471 [$\text{M} + \text{Na}^+$], calcd for $\text{C}_{30}\text{H}_{21}\text{NO}_2$ [M]: 427.1572.

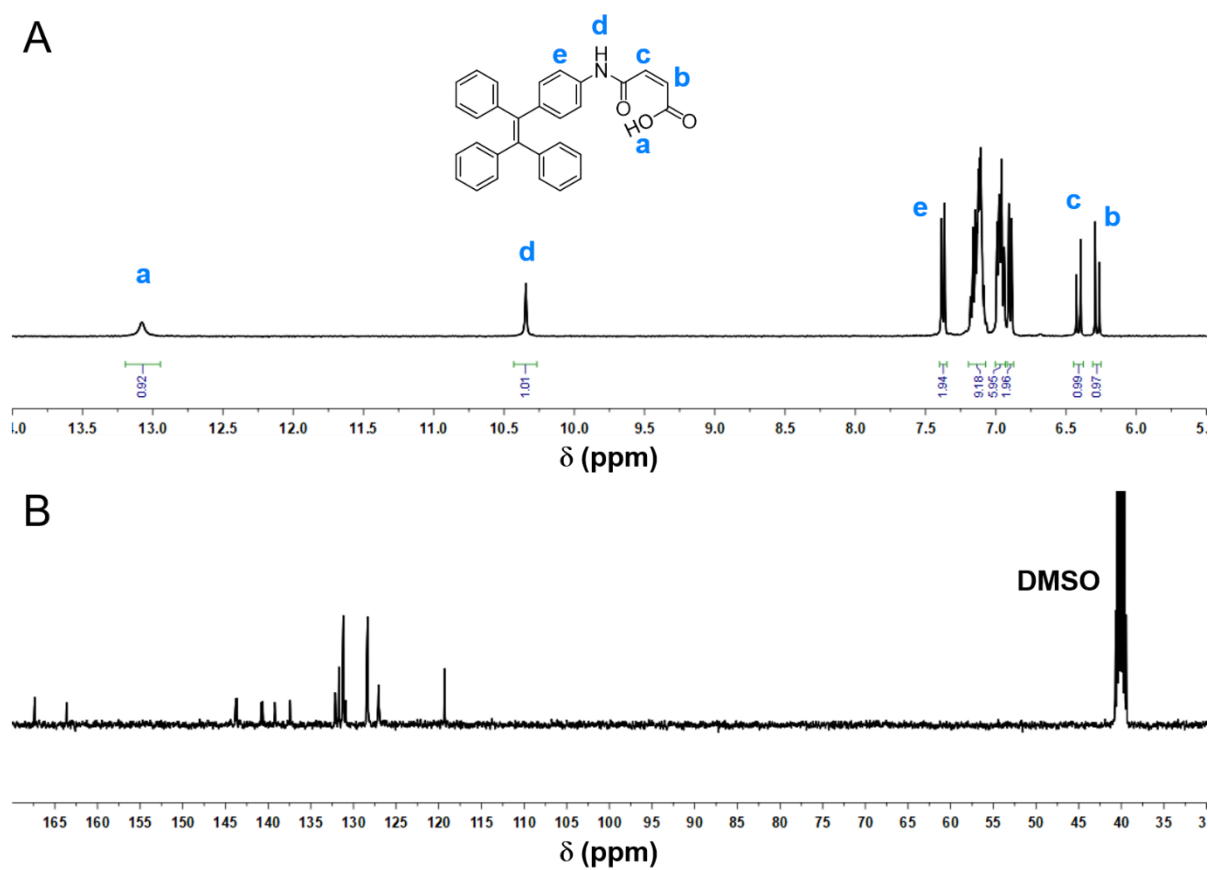


Figure S2. (A) ^1H and (B) ^{13}C NMR spectra of TPEX in $\text{DMSO-}d_6$ with corresponding assignments.

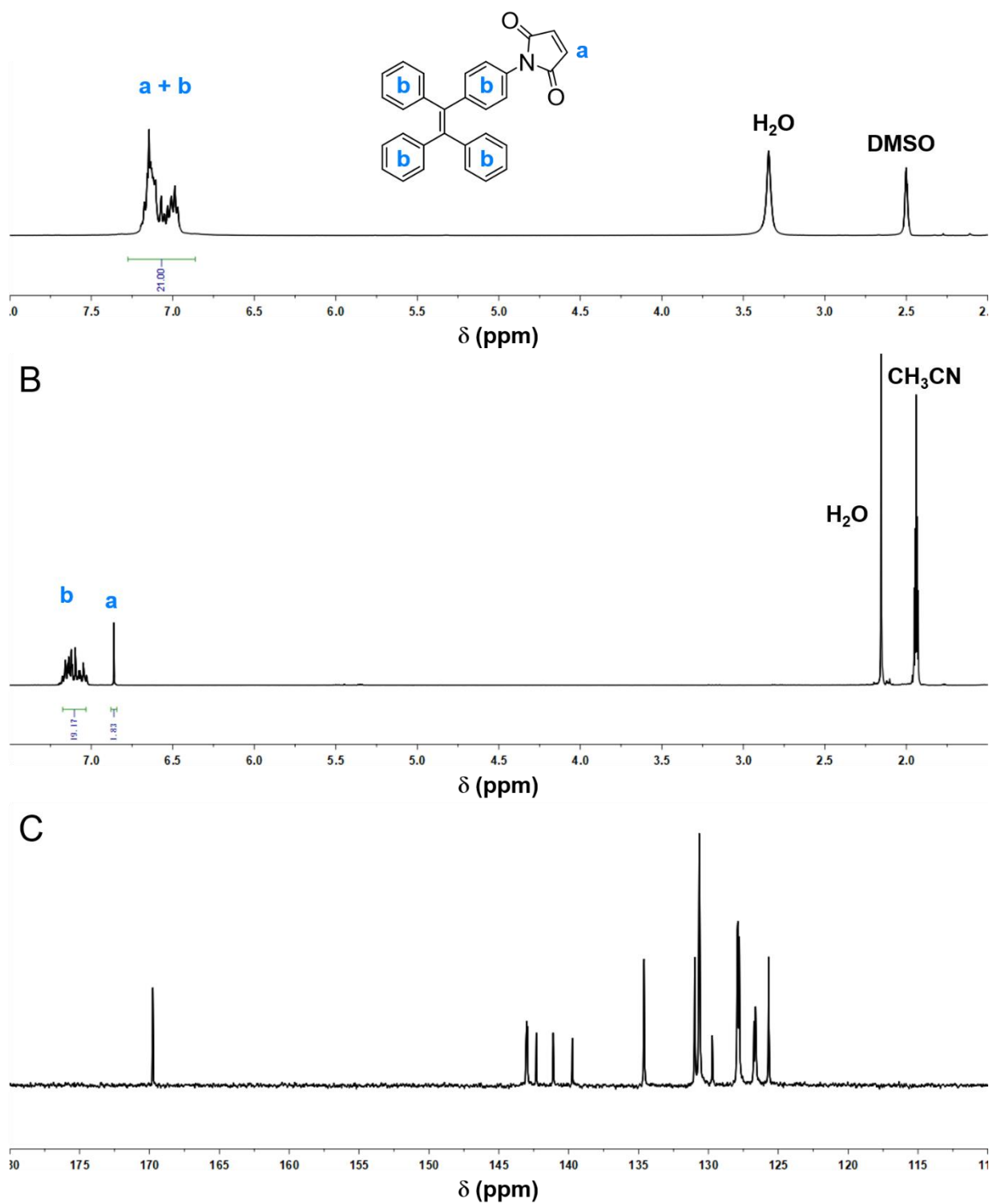


Figure S3. ^1H spectra of TPEMI in (A) $\text{DMSO}-d_6$ and (B) $\text{Acetonitrile}-d_3$ with corresponding assignments. (C) ^{13}C NMR spectra of TPEMI in $\text{DMSO}-d_6$.

(TPE-A)

In a round bottom flask, a solution of TPEMI (0.855 g, 2 mmol) and furfuryl alcohol (0.490 g, 5 mmol) in 10 mL dichloromethane was stirred at room temperature for 24 h. Then the mixture washed by brine, and the organic layer was filtered, concentrated and purified using column chromatography (silica gel, PE/DCM 100:50, v/v). The pure product was a light yellow solid with strong fluorescence (0.862 g, 82%).

^1H NMR (DMSO- d_6 , 400 MHz), δ (TMS, ppm): 7.17 - 6.95 (m, 18H), 6.92 - 6.89 (m, 1H), 6.58 - 6.43 (m, 2H), 5.30 (dd, J = 5.5, 1.4 Hz, 0.5H), 5.20 (t, J = 5.8 Hz, 0.5H, -OH), 5.15 (d, J = 1.2 Hz, 0.5H), 5.00 (t, J = 5.7 Hz, 0.5H, -OH), 4.10 - 3.90 (m, 1.5H), 3.78 - 3.71 (m, 1H), 3.52 (d, J = 7.7 Hz, 0.5H), 3.16 (d, J = 6.5 Hz, 0.5H), 2.98 (d, J = 6.6 Hz, 0.5H). ^1H NMR (ACETONITRILE- d_3 , 400 MHz), δ (TMS, ppm): 7.18 - 6.98 (m, 18H), 6.88 (d, J = 8.4 Hz, 1H), 6.62 - 6.38 (m, 2H), 5.32 - 5.16 (m, 1H), 4.04 (m, 2H), 3.71 - 3.48 (m, 1H), 3.18 - 2.93 (m, 2H). ^{13}C NMR (DMSO- d_6 , 400 MHz), δ (TMS, ppm): 175.46, 174.02, 143.02, 142.94, 142.87, 141.27, 139.70, 138.28, 136.60, 135.53, 135.28, 130.96, 130.64, 130.18, 127.94, 127.82, 126.79, 126.65, 126.15, 125.95, 92.74, 92.09, 80.63, 78.87, 59.51, 58.99, 50.23, 47.99, 47.71, 45.14. MS (ESI IT-TOF): m/z 548.1855 [$\text{M} + \text{Na}^+$], calcd for $\text{C}_{35}\text{H}_{27}\text{NO}_4$ [M]: 525.1940.

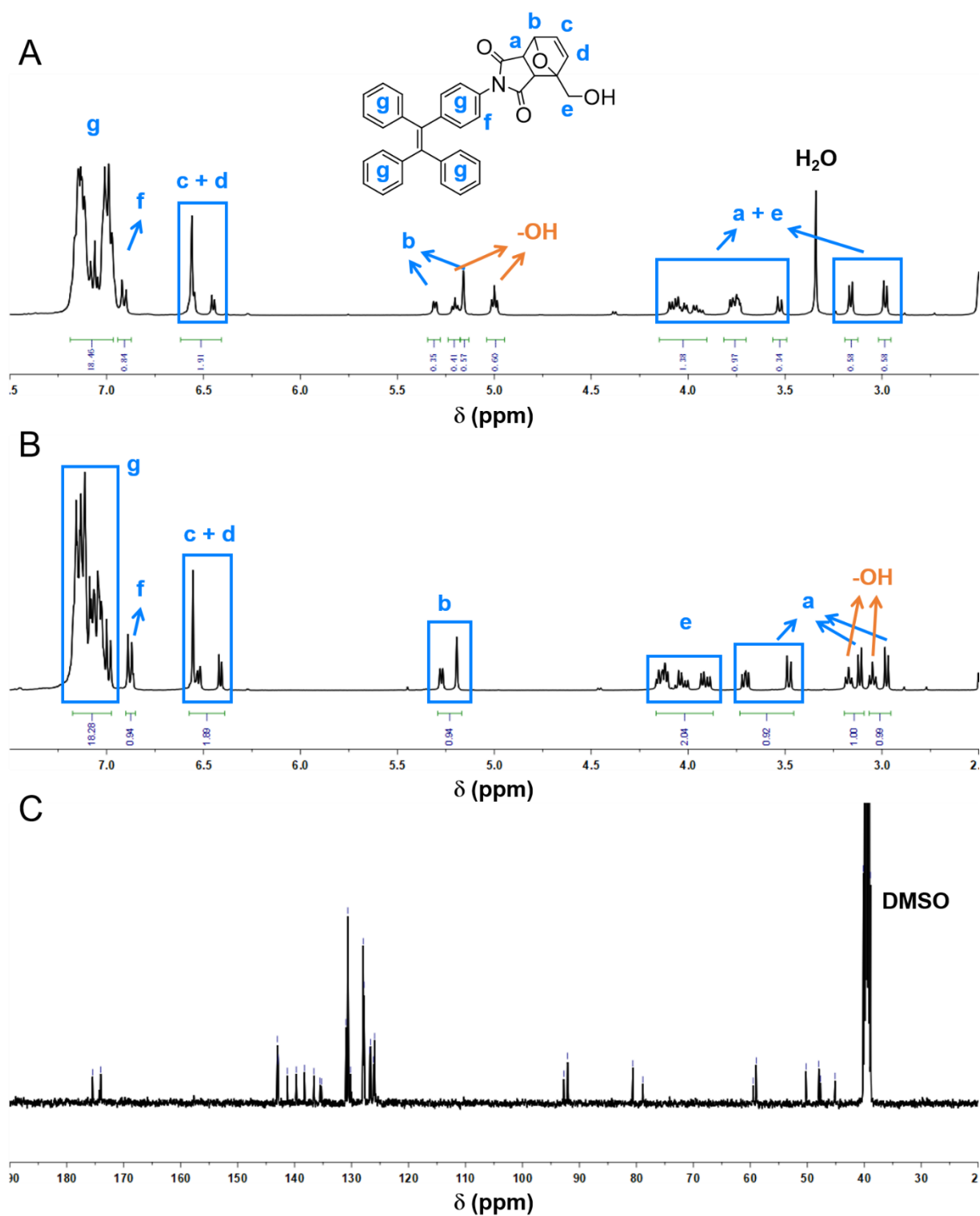


Figure S4. ^1H spectra of TPE-A in (A) $\text{DMSO-}d_6$ and (B) $\text{Acetonitrile-}d_3$ with corresponding assignments. (C) ^{13}C NMR spectra of TPE-A in $\text{DMSO-}d_6$.

(TPE-B)

In a round bottom flask, a solution of TPEMI (0.855 g, 2 mmol) and 3-furanmethanol (0.490 g, 5 mmol) in 10 mL dichloromethane was stirred at room temperature for 24 h. Then the mixture washed by brine, and the organic layer was filtered, concentrated and purified using column chromatography (silica gel, PE/DCM 100:50, v/v). The pure product was a light yellow solid with strong fluorescence (0.915 g, 87%).

^1H NMR (DMSO- d_6 , 400 MHz), δ (TMS, ppm): 7.17 - 6.94 (m, 17H), 6.87 (d, J = 8.4 Hz, 2H), 6.14 (d, J = 1.3 Hz, 1H), 5.32 - 5.23 (m, 2H), 5.13 - 5.07 (m, 1H), 4.12 - 3.93 (m, 2H), 3.72 - 3.62 (m, 2H). ^1H NMR (ACETONITRILE- d_3 , 400 MHz), δ (TMS, ppm): 7.18 - 7.01 (m, 17H), 6.90 - 6.84 (m, 2H), 6.18 (d, J = 1.8 Hz, 1H), 5.27 (d, J = 2.4 Hz, 1H), 5.19 (d, J = 3.1 Hz, 1H), 4.22 (d, J = 15.2 Hz, 1H), 4.03 (dd, J = 16.3, 2.9 Hz, 1H), 3.68 - 3.60 (m, 2H), 3.10 (t, J = 4.9 Hz, 1H). ^{13}C NMR (ACETONITRILE- d_3 , 100 MHz), δ (TMS, ppm): 175.36, 174.94, 151.84, 144.94, 144.41, 144.35, 144.30, 142.80, 140.95, 132.29, 131.75, 131.70, 131.66, 131.22, 128.84, 128.78, 128.65, 127.69, 127.58, 127.53, 127.22, 81.03, 80.52, 59.28, 48.32, 47.04. MS (ESI IT-TOF): m/z 548.1854 [$\text{M} + \text{Na}^+$], calcd for $\text{C}_{35}\text{H}_{27}\text{NO}_4$ [M]: 525.1940.

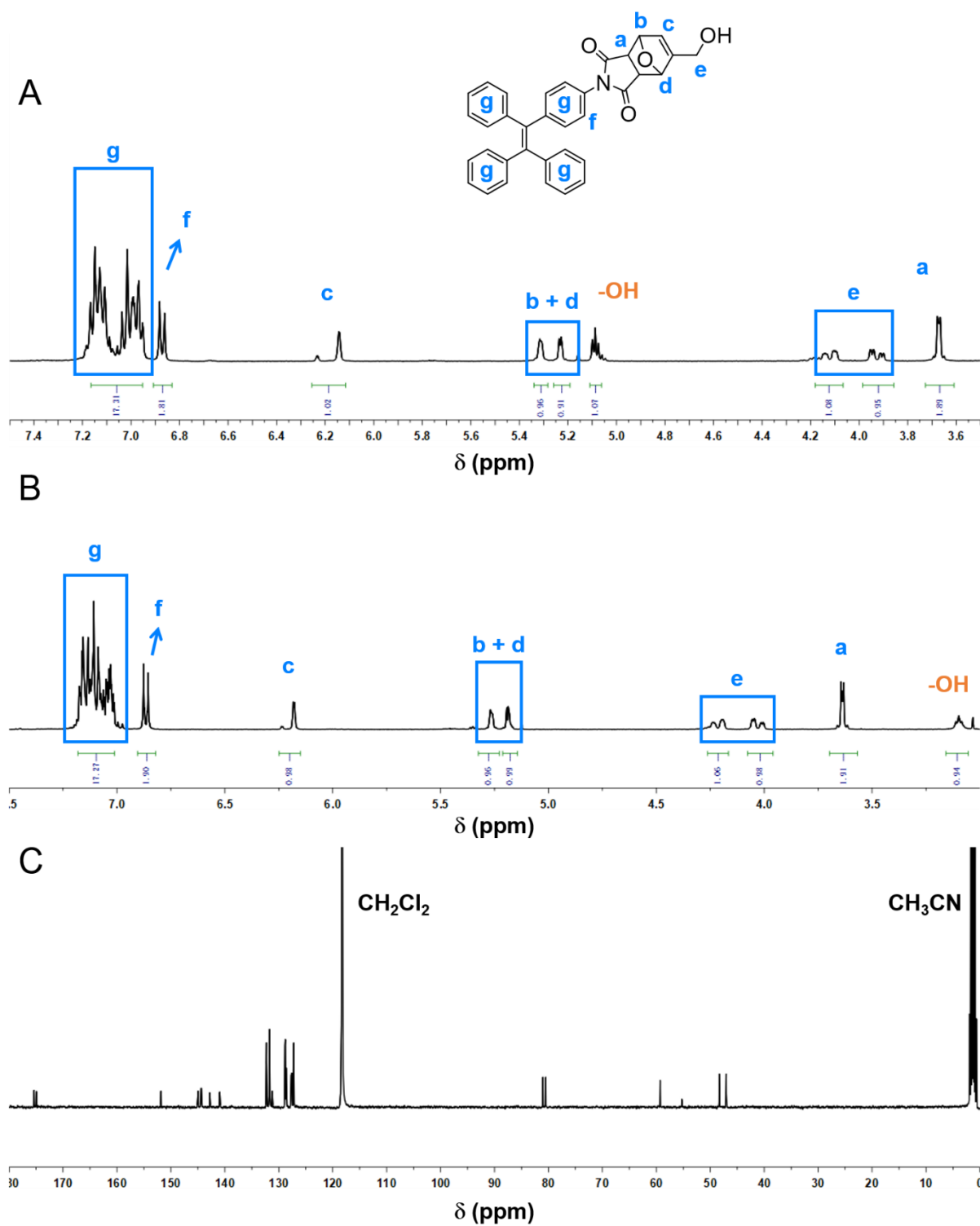


Figure S5. ¹H spectra of TPE-B in (A) DMSO-*d*₆ and (B) Acetonitrile-*d*₃ with corresponding assignments. (C) ¹³C NMR spectra of TPE-B in Acetonitrile-*d*₃.

(TPE-C)

In a round bottom flask, a solution of TPEMI (0.855 g, 2 mmol) and 2,5-furandimethanol (0.640 g, 5 mmol) in 10 mL CH₃CN was stirred at room temperature for 24 h. Then the mixture washed by brine, and the organic layer was filtered, concentrated and purified using column chromatography (silica gel, PE/DCM 50:50, v/v). The pure product was a light yellow solid with strong fluorescence (0.789 g, 71%)

¹H NMR (DMSO-*d*₆, 400 MHz), δ (TMS, ppm): 7.19 - 7.09 (m, 9H), 7.06 - 6.95 (m, 8H), 6.91 (d, *J* = 8.4 Hz, 2H), 6.45 (s, 2H), 5.20 (t, *J* = 5.7 Hz, 2H), 4.01 (dd, *J* = 12.8, 5.4 Hz, 2H), 3.91 (dd, *J* = 12.8, 6.0 Hz, 2H), 3.62 (s, 2H). ¹H NMR (ACETONITRILE-*d*₃, 400 MHz), δ (TMS, ppm): 7.17 - 7.02 (m, 17H), 6.88 (d, *J* = 8.1 Hz, 2H), 6.44 (s, 2H), 4.15 - 4.08 (m, 2H), 4.06 - 3.97 (m, 2H), 3.58 (s, 2H), 3.18 (t, *J* = 5.9 Hz, 2H). ¹³C NMR (DMSO-*d*₆, 100 MHz), δ (TMS, ppm): 174.37, 143.03, 142.97, 142.87, 141.22, 139.67, 136.12, 130.93, 130.62, 130.07, 127.98, 127.94, 127.83, 126.80, 126.66, 126.15, 92.55, 59.69, 47.23. MS (ESI IT-TOF): *m/z* 578.1968 [M + Na⁺], calcd for C₃₆H₂₉NO₅ [M]: 555.2046.

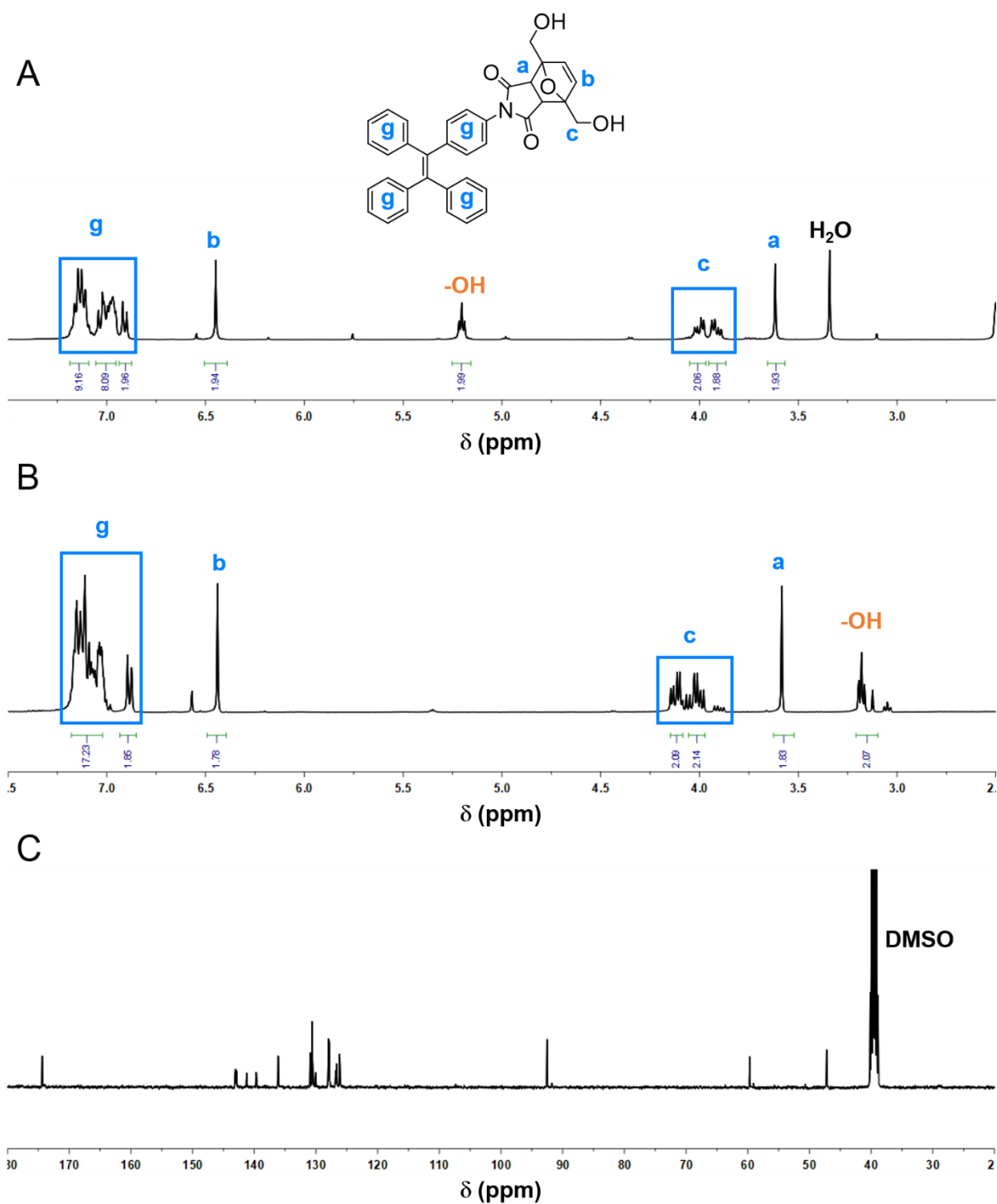


Figure S6. ^1H spectra of TPE-C in (A) $\text{DMSO}-d_6$ and (B) $\text{Acetonitrile}-d_3$ with corresponding assignments. (C) ^{13}C NMR spectra of TPE-C in $\text{DMSO}-d_6$.

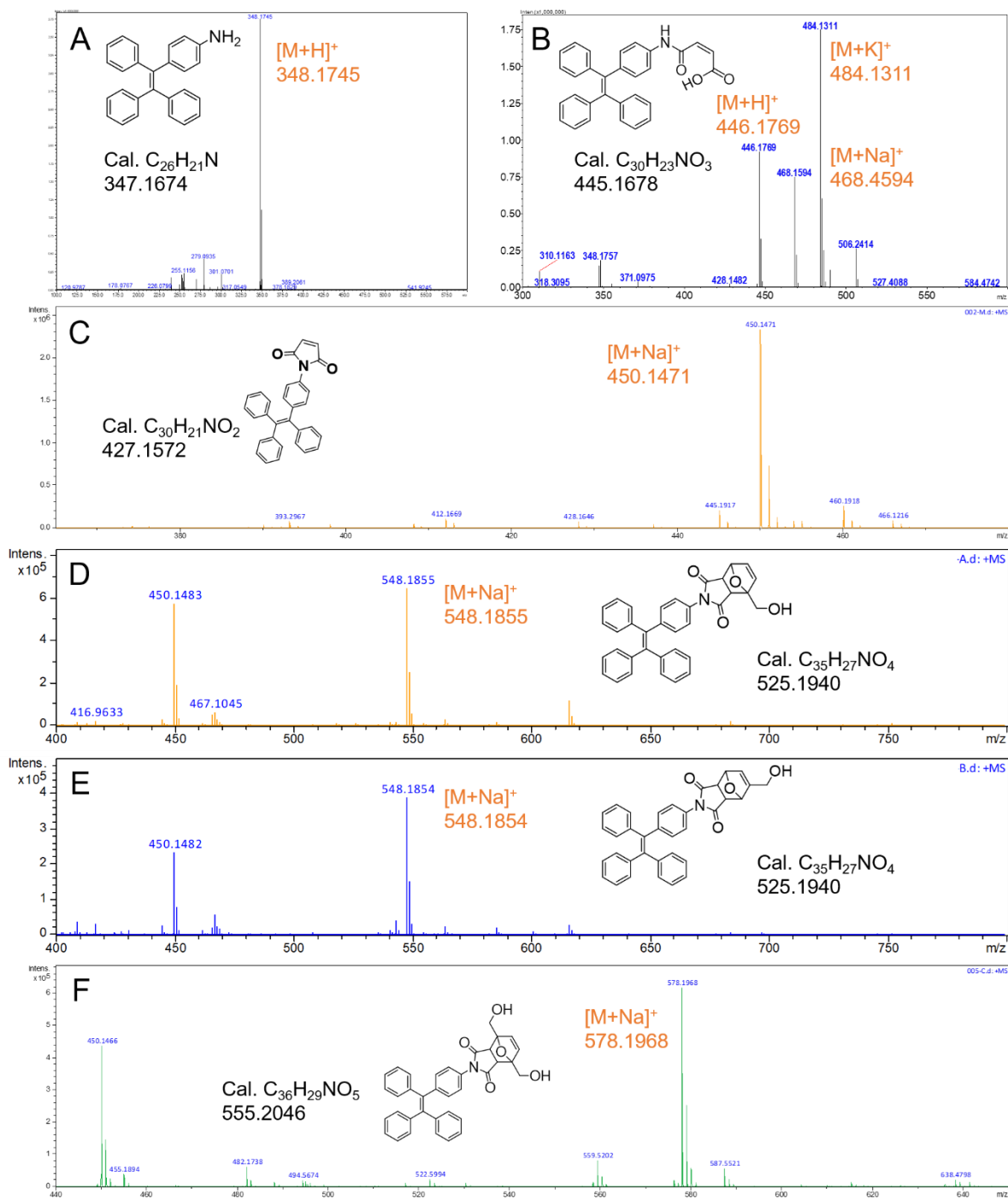


Figure S7. High-resolution mass spectra of (A) TPEAM, (B) TPEX, (C) TPEMI, (D) TPE-A, (E) TPE-B, and (F) TPE-C. The theoretical calculations are shown in black and experimental results in orange.

X-ray single-crystal diffraction structure analysis

To investigate the structure of the core molecule, TPEMI, we prepared its high-quality organic single crystal and analyzed the results (Figure S8). The single crystal diffraction data showed the structure belonged to triclinic system with cell parameters of $a = 9.48 \text{ \AA}$, $b = 10.82 \text{ \AA}$, $c = 23.10 \text{ \AA}$, $\alpha = 92.78^\circ$, $\beta = 92.46^\circ$, $\gamma = 105.66^\circ$ and $V = 2273.81 \text{ \AA}^3$. The crystal density of TPEMI was 1.249 g/cm^3 and the space group was P-1.

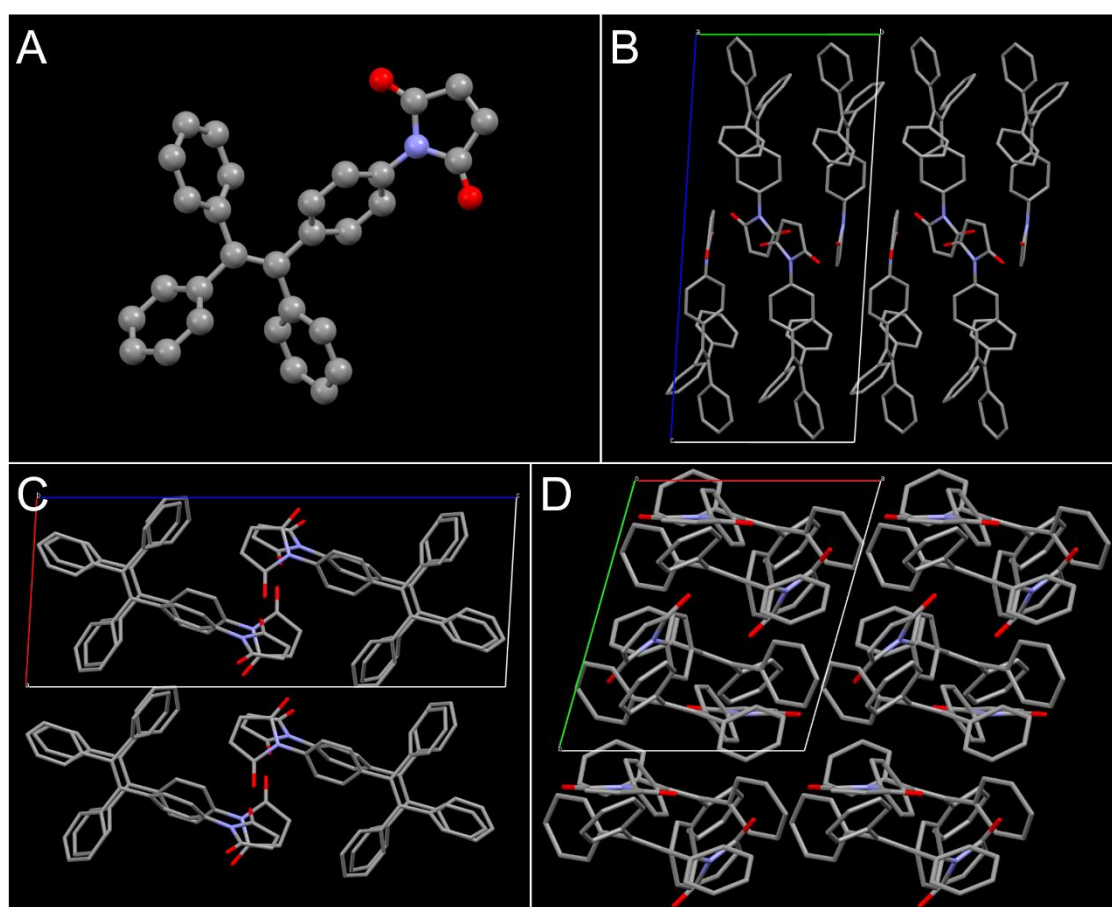


Figure S8. X-ray single-crystal diffraction structure analysis. (A) Molecular structure (ORTEP diagram) of TPEMI determined by single crystal X-ray diffraction with ball and stick. Crystal packing diagrams of TPEMI along (B) the a-axis, (C) the b-axis, and (D) the c-axis. All hydrogen atoms are omitted for clarity.

3. Optical characterization

The optical properties of TPEMI and TPE-DAs were characterized first, which is the basis for their use in the visualization of reversible DA/RDA reactions.

As shown in Figure S9A, TPE-DAs and TPEMI share similar UV-Vis absorption. The absorption maximum at around 300 nm is assigned to the π - π^* electron transition of aromatic rings and n - π^* electron transition of carbonyl groups. Excited at 300 nm, the fluorescence spectra of TPEMI and TPE-DAs were recorded. It was obvious that TPEMI was non-emissive while TPE-DAs were all AIE-active, which could be well explained by the existence of the n - π electronic conjugation of the carbonyl (C=O) and olefinic (C=C) groups in maleimide (Figure S9B-S9E). When the fraction of water in CH₃CN/water mixture increased from 10% to 90%, the fluorescent intensities increased by 260, 570 and 275 times for TPE-A, TPE-B and TPE-C, respectively (Figure S9F). The photo of TPEMI and TPE-DAs in both good solvents and aqueous mixtures were shown in Figure S10. The TEM and DLS results also supported the formation of the aggregates in $f_w = 90\%$ DMSO/water dispersions (Figure S11). The difference between TPE-A and TPE-B was confirmed with their fluorescence quantum yields, which is a key factor for monitoring DA exchange reactions with the fluorescence method.

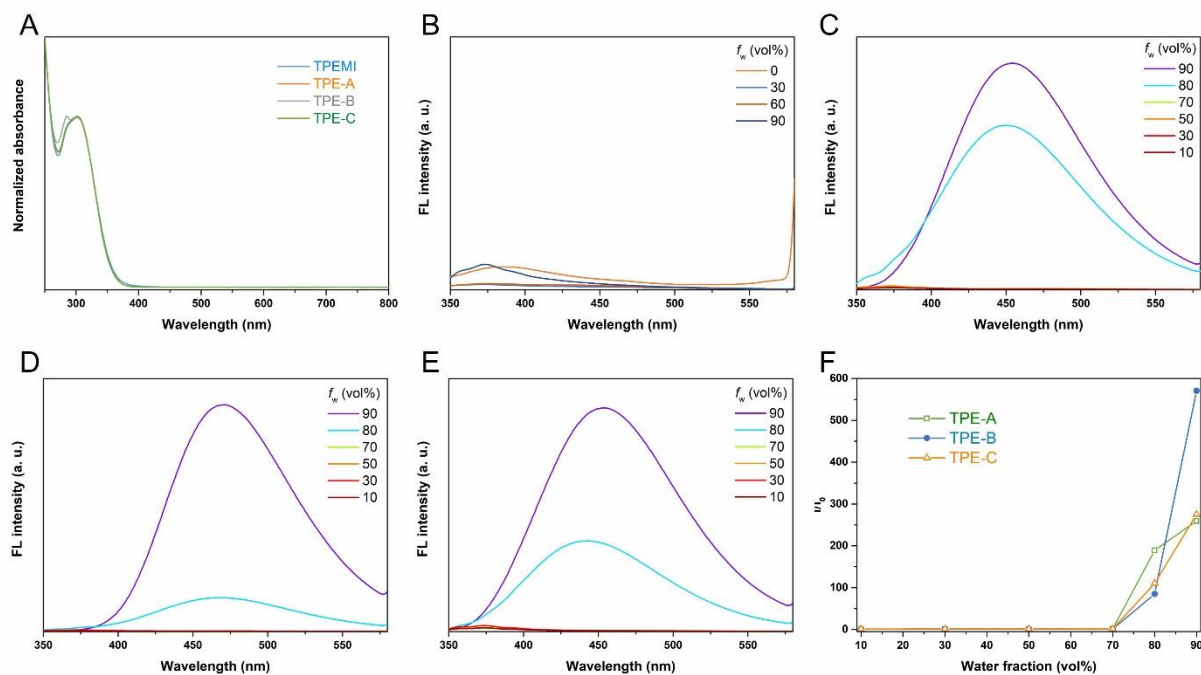


Figure S9. UV-Vis absorption and emission properties of TPEMI and TPE-DAs. (A) UV-Vis absorption in CH₃CN at 100 μM. Emission spectra of (B) TPEMI, (C) TPE-A, (D) TPE-B, and (E) TPE-C at 100 μM in CH₃CN/water mixtures with different water fractions (f_w). (F) The plot of relative fluorescence intensity (I/I_0) versus water fractions ($\lambda_{ex} = 300$ nm, I_0 is the fluorescence intensity in CH₃CN/water mixtures with $f_w = 10\%$).

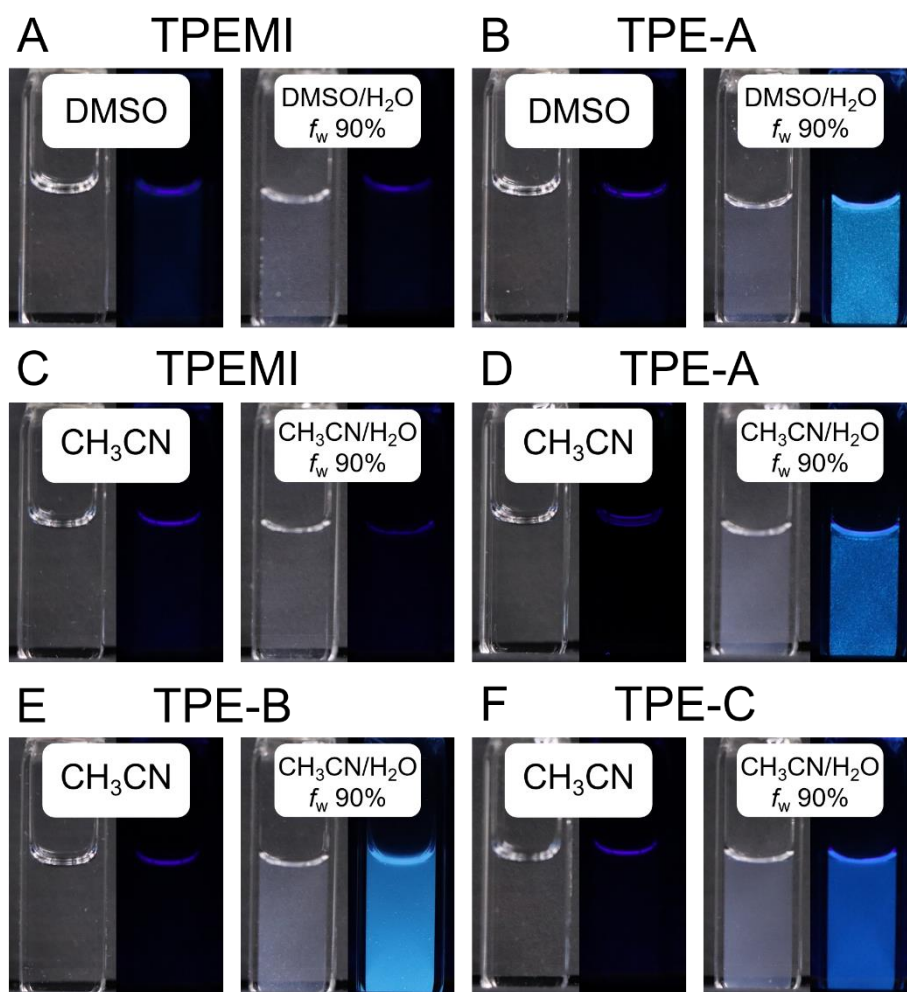


Figure S10. Photos of 100 μ M TPEMI and TPE-DAs in both good solvents and aqueous mixtures under visible light and UV light (365 nm): (A) TPEMI and (B) TPE-A in DMSO and DMSO/water ($f_w = 90\%$), (C) TPEMI, (D) TPE-A, (E) TPE-B, and (F) TPE-C in CH₃CN and CH₃CN/water ($f_w = 90\%$).

Table S1. Spectral and photophysical data of the TPE-DAs.

		Excitation maximum ($\lambda_{\text{ex,max}}$), nm	Emission maximum ($\lambda_{\text{em,max}}$), nm	Stokes shift, nm	Quantum yields (QY)*
TPE-A	CH ₃ CN/water ($f_w = 90\%$)	302	451	149	0.17
	DMSO/water ($f_w = 90\%$)	323	472	149	
TPE-B	CH ₃ CN/water ($f_w = 90\%$)	323	467	144	0.49
	DMSO/water ($f_w = 90\%$)	323	472	149	
TPE-C	CH ₃ CN/water ($f_w = 90\%$)	302	451	149	0.24
	DMSO/water ($f_w = 90\%$)	289	436	147	

*The fluorescence quantum yields were measured in powder.

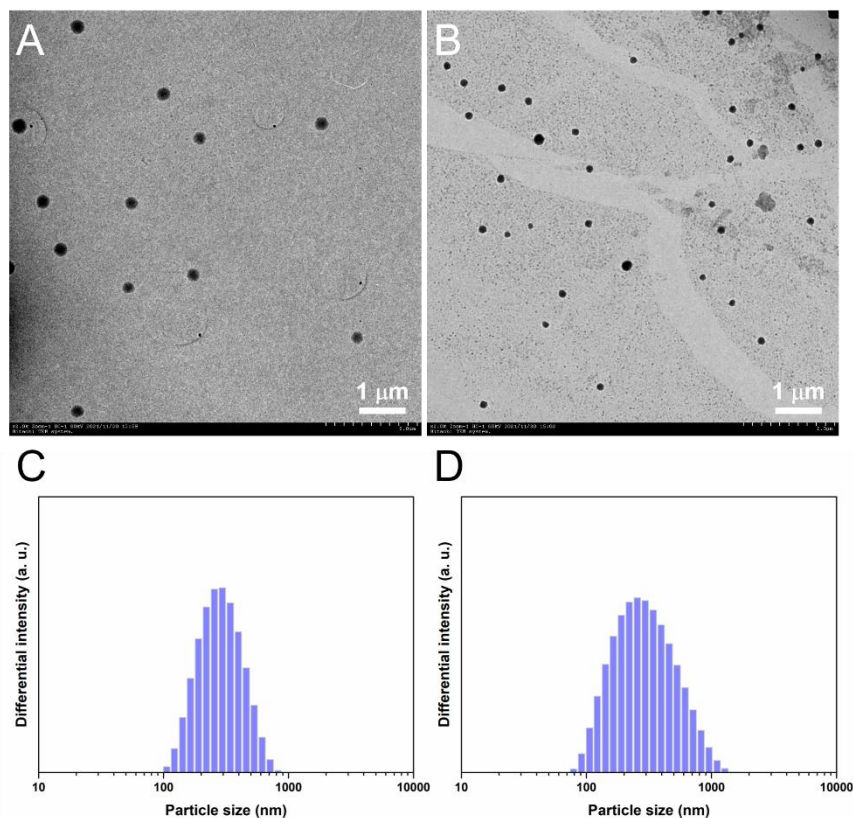


Figure S11. TEM image of (A) TPEMI and (B) TPE-A aggregates; scale bar: 1 μm . DLS results of (C) TPEMI and (D) TPE-A at 100 μM in DMSO/water dispersions ($f_w = 90\%$).

4. Intermolecular quenching effect in DA reaction mixture

To verify the universality of TPEMI quenching effect, similar to the TPEMI/TPE-A mixture, TPEMI was mixed with TPE-B and TPE-C, respectively, at gradient molar ratios (0/10, 1/9, 2/8, 3/7, 4/6, 5/5, 6/4, 7/3, 8/2, 9/1, 10/0, and total concentration of TPEMI and TPE-DAs was 100 $\mu\text{mol/L}$). The fluorescence spectra and the corresponding plots were obtained (Figure S12). As is expected, the relation between the relative fluorescence intensity and the fraction of TPEMI was also exponential for TPE-B and TPE-C, and their variances R^2 were 0.998 and 0.998, respectively. In conclusion, the relation between the relative fluorescence intensity and the contents of TPEMI/TPE-DAs mixtures can be described with an exponential function qualitatively and quantitatively.

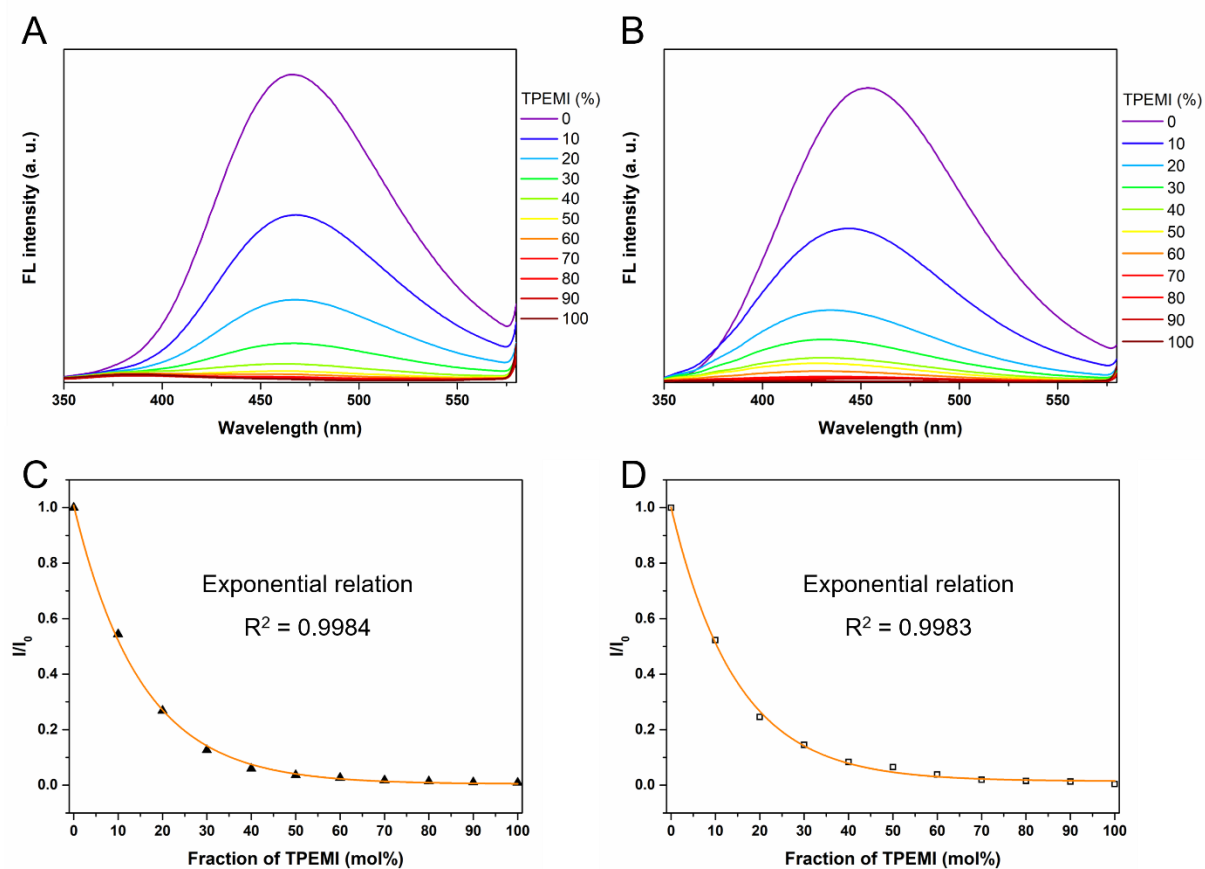


Figure S12. Intermolecular quenching effect of TPEMI. Fluorescence spectra of TPEMI mixed with (A) TPE-B and (B) TPE-C in $\text{CH}_3\text{CN}/\text{water}$ ($f_w = 90\%$) with different fraction of TPEMI from 0% (top) to 100% (bottom). The total concentration is 100 μM . The plots of relative fluorescence intensity (I/I_0) at λ_{em} versus fraction of TPEMI in mixture (C) TPE-B/TPEMI and (D) TPE-C/TPEMI ($\lambda_{\text{ex}} = 300 \text{ nm}$).

As shown in Figure S13, the influence of the chosen good solvents was investigated in both DMSO/water and THF/water mixtures ($f_w = 90\%$), and the relation between the relative fluorescence intensity and the fraction of TPEMI was also exponential with R^2 were 0.999 and 0.987, respectively.

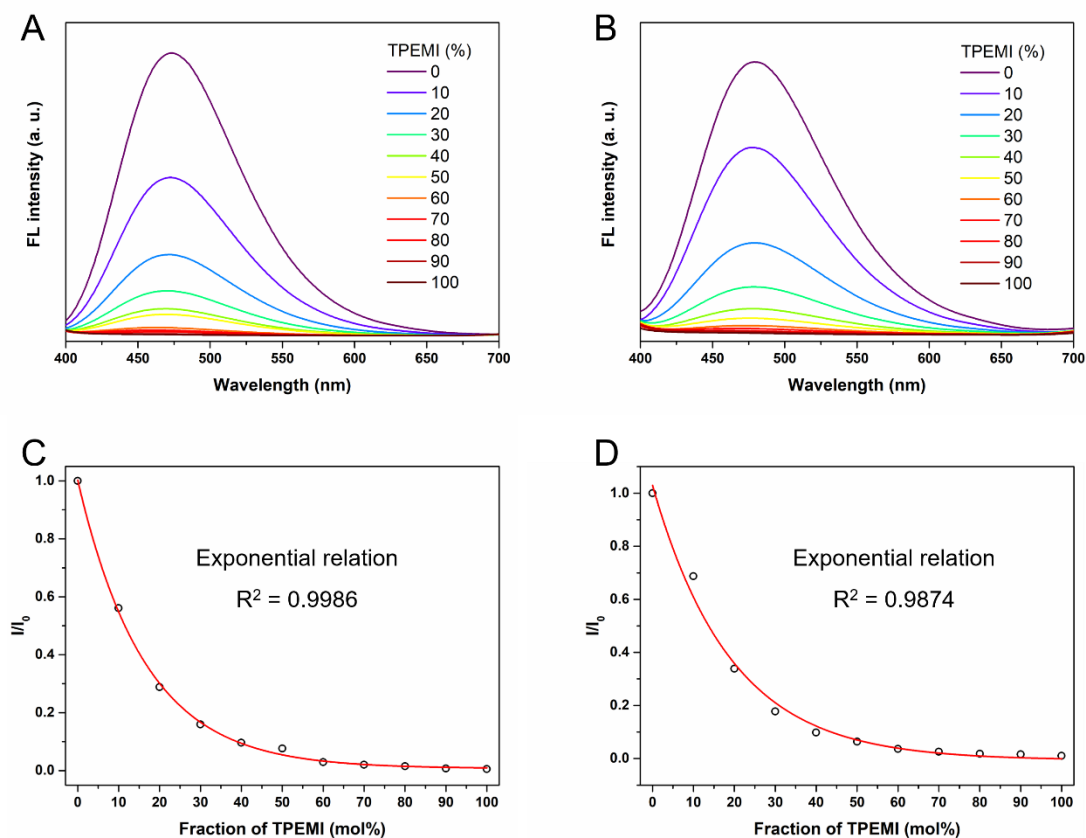


Figure S13. Inter-molecular quenching effect of TPEMI. Fluorescence spectra of TPEMI mixed with TPE-A in (A) DMSO/water and (B) THF/water ($f_w = 90\%$) with different fraction of TPEMI from 0% (top) to 100% (bottom). The total concentration is 100 μM . The plots of relative fluorescence intensity (I/I_0) at λ_{em} versus fraction of TPEMI in mixture of (C) DMSO/water and (D) THF/water ($\lambda_{\text{ex}} = 365 \text{ nm}$).

To ensure the application of TPEMI/TPE-DAs systems in actual DA/RDA reactions, the fluorescence influence of the other reactant, furan derivatives, was verified first. Taking furfuryl alcohol as an example, in CH₃CN/water ($f_w = 90\%$) solution, 100 $\mu\text{mol/L}$ TPE-A was mixed with a gradient concentration of furfuryl alcohol. As shown in Figure S14, fluorescence intensities nearly did not change with the increase of furfuryl alcohol.

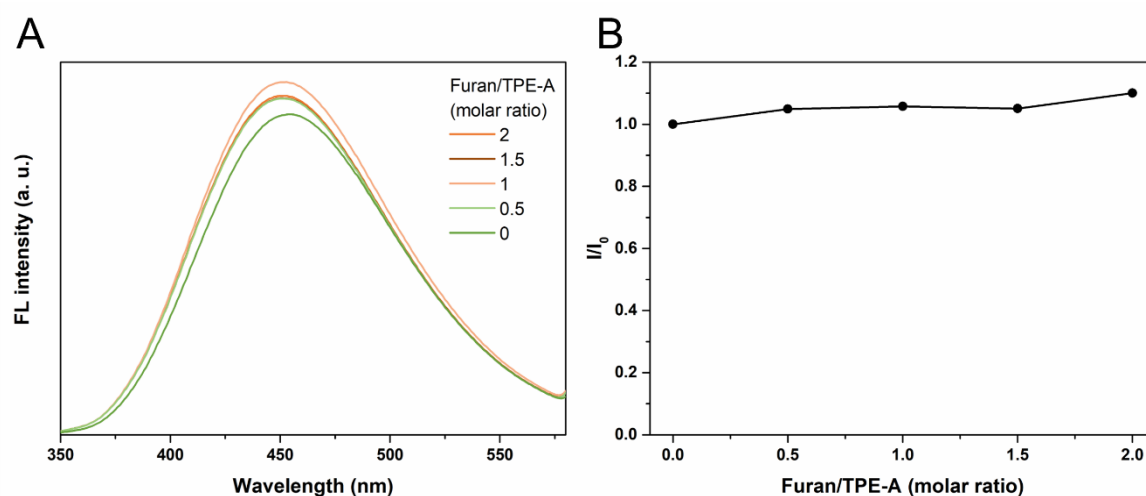


Figure S14. Effect of the reactant, furan derivatives (furfuryl alcohol as the example) on the fluorescence behavior. (A) Fluorescence spectra of furfuryl alcohol and TPE-A mixture in CH₃CN/water ($f_w = 90\%$) with different concentrations of furfuryl alcohol (0, 50, 100, 150 and 200 μM). (B) The plot of relative fluorescence intensity (I/I_0) at λ_{em} versus the molar ratio of furfuryl alcohol and TPE-A ($\lambda_{\text{ex}} = 300 \text{ nm}$, the concentration of TPE-A is 100 μM).

To confirm the applicability of the quantitative relation, Equation (5), between the fluorescence intensity and concentration of TPEMI, a group of relative fluorescence intensity (I/I_0) values were calculated with the variates TPEMI/TPE-A (the same conditions as in Figure 2B). As shown in Figure S15, the experiment results from Figure 2B (orange solid points) can be well fitted by the calculated values (green hollow triangles), and the K_F was 22.8. The good coincidence between the calculated and experimental values illustrated the reasonability of quantitative equations. In addition, the relation between calculated values I/I_0 and fraction of TPEMI was exponential and R^2 was 0.9908, which also identified the applicability of the qualitative relation, Empirical correlation (1).

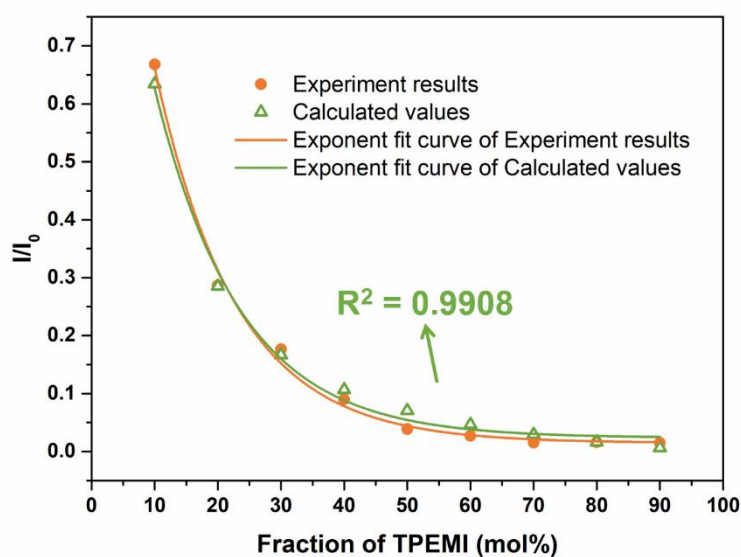


Figure S15. Verification of quantitative equation. The green hollow triangles were relative fluorescence intensity calculated values from Equation (5), the orange solid points were experiment results. The R^2 of the green dots fitted by the exponential function is 0.9908.

5. Kinetics of reversible DA reaction

Having established the qualitative and quantitative relation between the fluorescence and the concentration ratio of TPE-DAs/TPEMI, we applied this fluorescence system in real DA reactions and attempted to monitor the reaction processes quantitatively. To investigate the kinetics of the reaction, both DA and RDA reactions were monitored with fluorescence spectroscopy and ^1H NMR. During the reactions 0.05 M TPEMI and furfuryl alcohol at 40 °C in CD_3CN , both two diastereomers (endo/exo adducts) of TPE-A were found in the NMR spectrum. As shown in Figure S16, the NMR peaks of the protons of TPE-A at δ 6.91-6.87 ppm (1H, H_f), δ 6.60-6.40 ppm (2H, H_c and H_d), δ 5.32-5.16 ppm (1H, H_b) and δ 4.20-2.95 ppm (5H, H_a , H_e and -OH) appeared and increased continuously. According to the changes at δ = 6.865-6.855 ppm and 6.910-6.870 ppm, the conversion table was obtained. The reaction reached equilibrium in about 24 h and at this point, the conversion is 95%. The DA processes can also be visualized in the CH_3CN /water (f_w = 90%) mixture with naked eyes as shown in Figure S17.

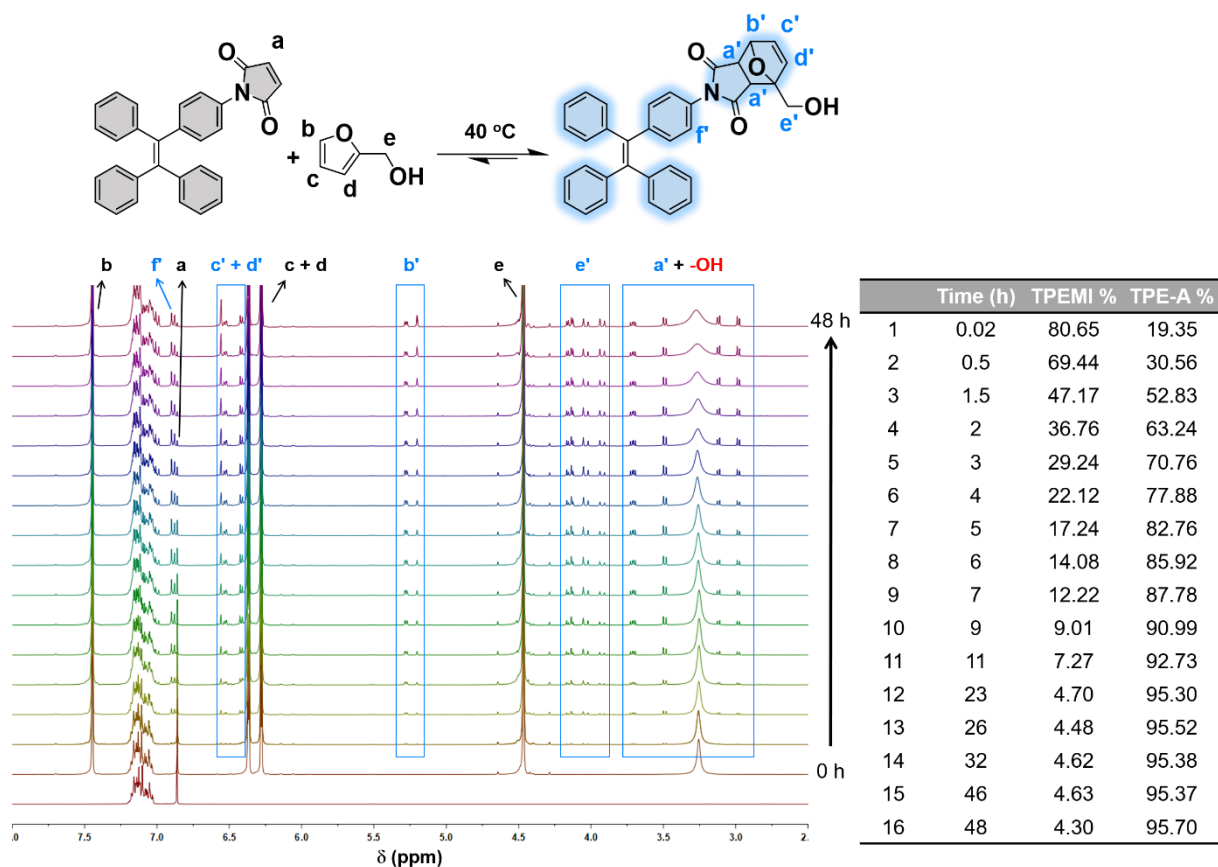


Figure S16. ^1H NMR spectral changes during TPE-A formation by the DA reaction at room temperature from 0 (bottom) to 48 h (top). The conversion table was calculated according to the changes at $\delta = 6.865\text{--}6.855$ ppm and $6.910\text{--}6.870$ ppm.

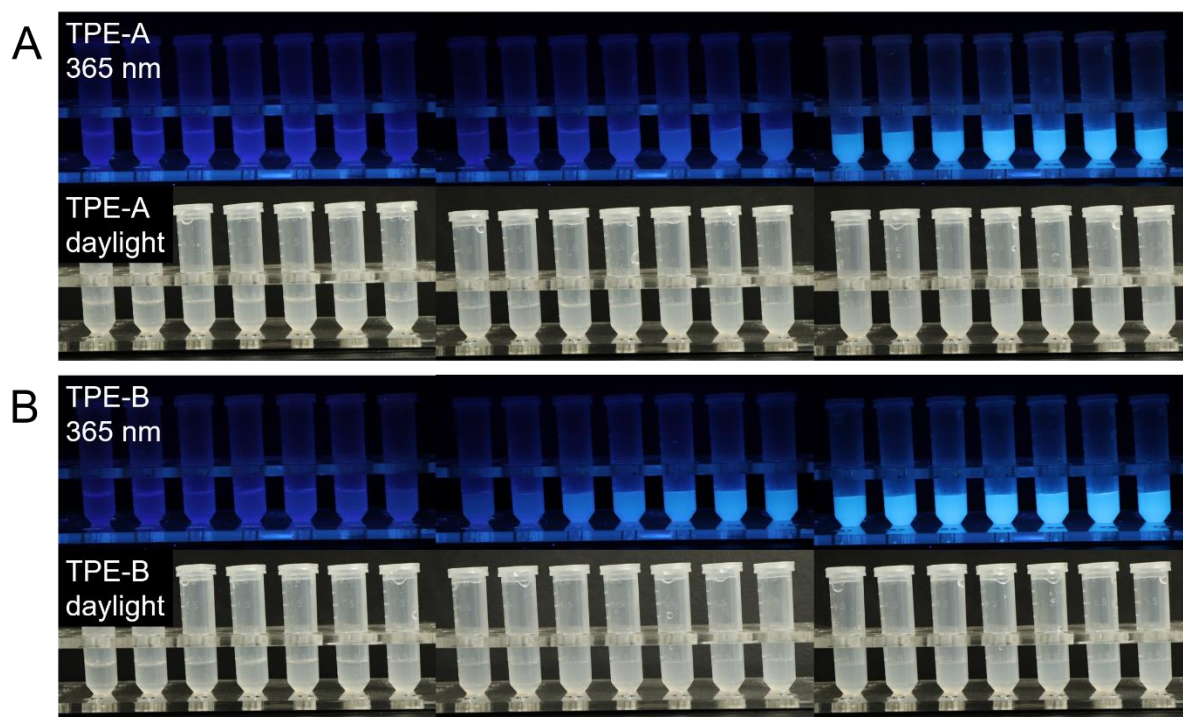


Figure S17. Photos during (A) TPE-A and (B) TPE-B formation by the DA reactions under UV light (365 nm) and visible light.

As the RDA reaction occurrence indicator, the fluorescence behaviors of TPE-A/TPEMI were investigated at 60 and 70 °C in CH₃CN (Figure S18). Heated at 60 °C, the fluorescence of the mixture changed slowly, the relative intensity decreased by 10% within 30 min and by 90% in 5 h. In addition, ¹H NMR was used to identify the production of TPEMI and furfuryl alcohol. As shown in Figure S19, during the RDA reactions of 0.05 M TPE-A, the peaks of furfuryl alcohol gradually appeared (δ 7.44 ppm (H_b), δ 6.38-6.25 ppm (H_c and H_d), δ 4.49-4.43 ppm (H_e) in CD₃CN, δ 7.57 ppm (H_b), δ 6.40-6.25 ppm (H_c and H_d), δ 4.40-4.35 ppm (H_e) in DMSO-*d*₆).

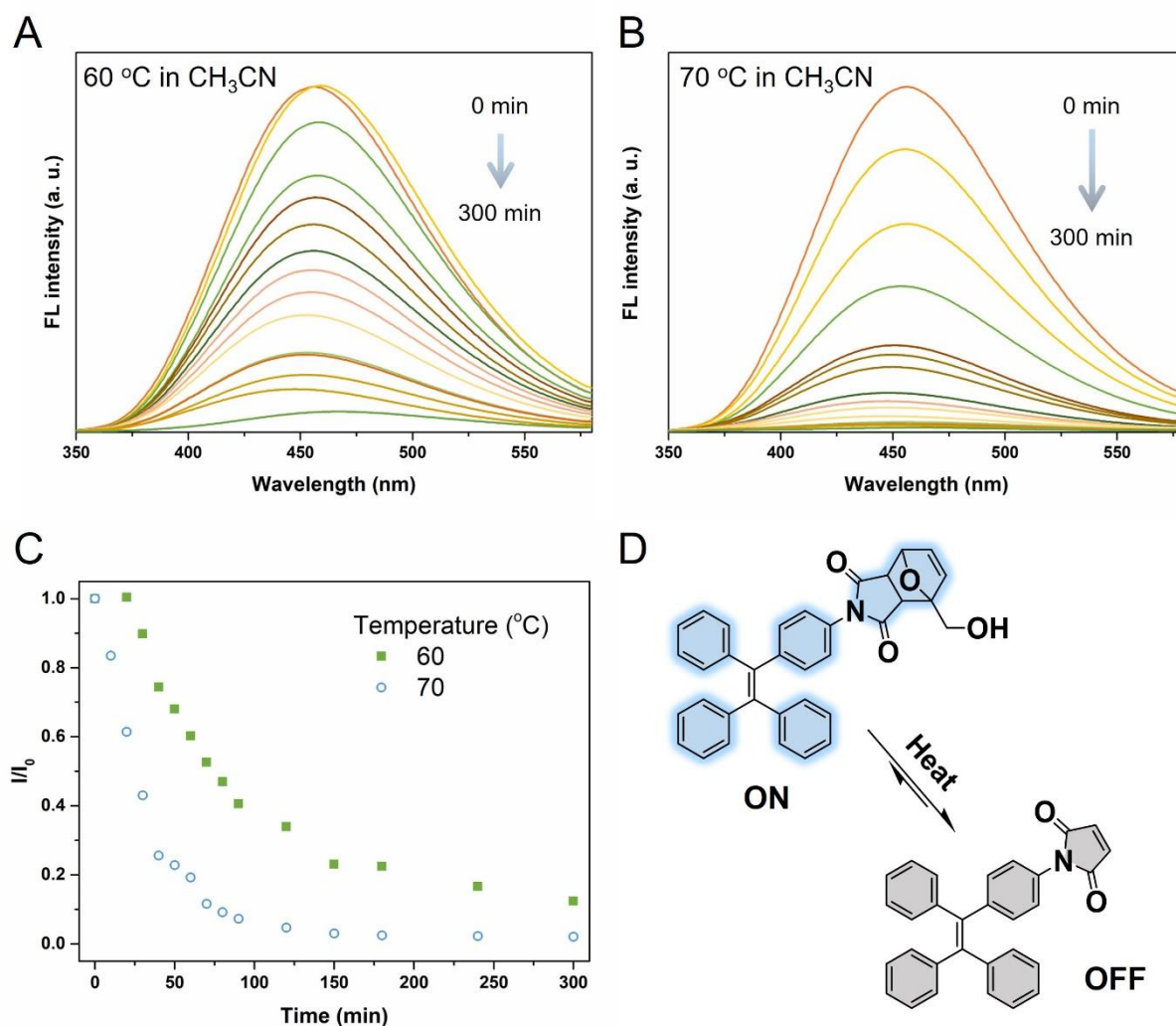


Figure S18. Fluorescence kinetics of TPE-A to TPEMI conversion via RDA reactions. Fluorescence spectra during TPE-A decomposition and TPEMI formation by the RDA reactions at (A) 60 °C and (B) 70 °C in CH₃CN from 0 (top) to 300 min (bottom). (C) The RDA reaction kinetics of TPE-A monitored by fluorescence spectroscopy according to relative intensity changes at λ_{em} . (D) Scheme of the RDA reactions. (Fluorescence spectra tested in CH₃CN/water solution with $f_w = 90\%$, $\lambda_{ex} = 300$ nm)

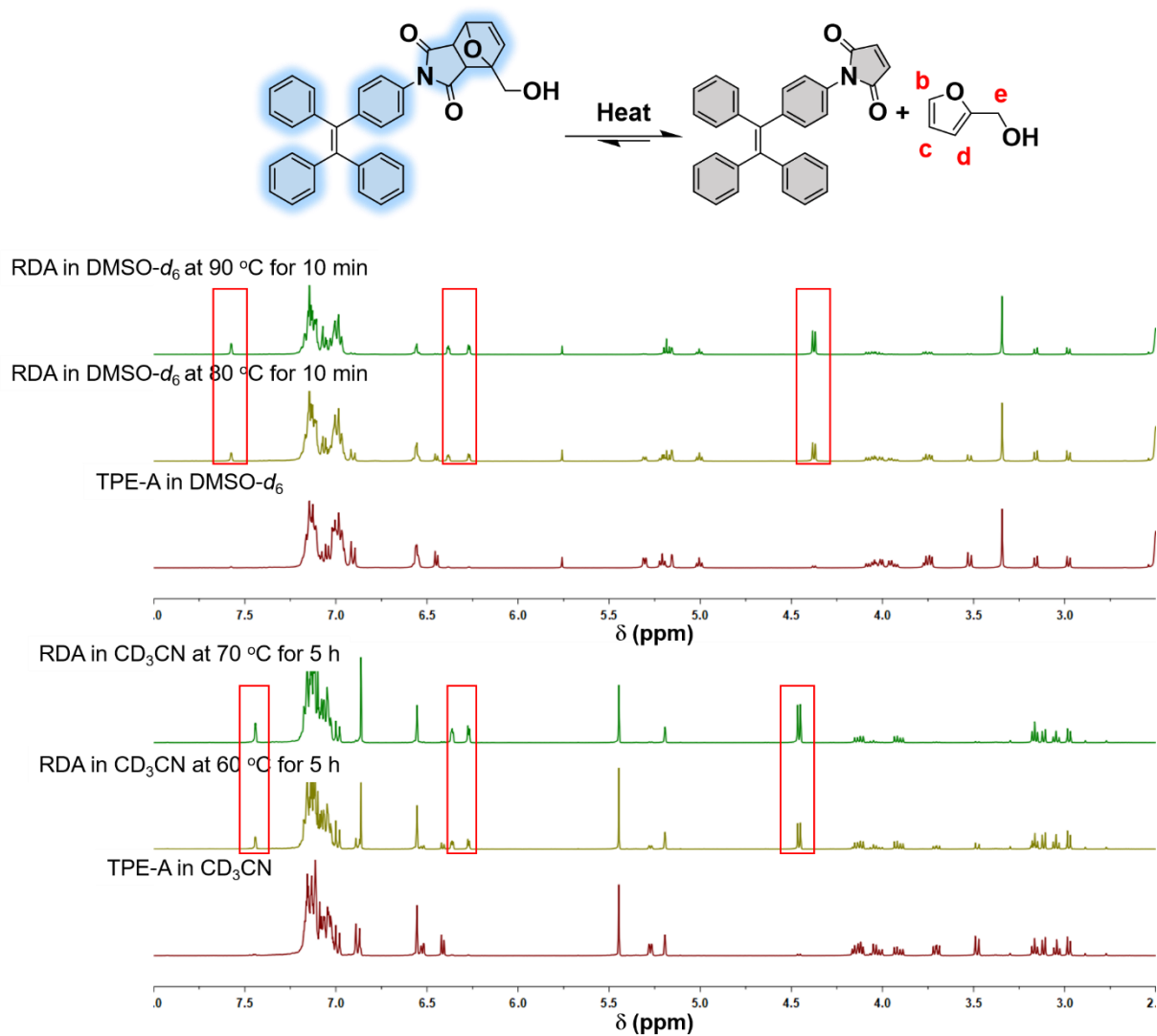


Figure S19. ¹H NMR spectral changes during TPE-A decomposition and TPEMI formation by the RDA reactions under different temperatures (60-70 °C in Acetonitrile-*d*₃, 80-90 °C in DMSO-*d*₆).

6. Heterogeneous DA reaction and RDA reaction on solid state

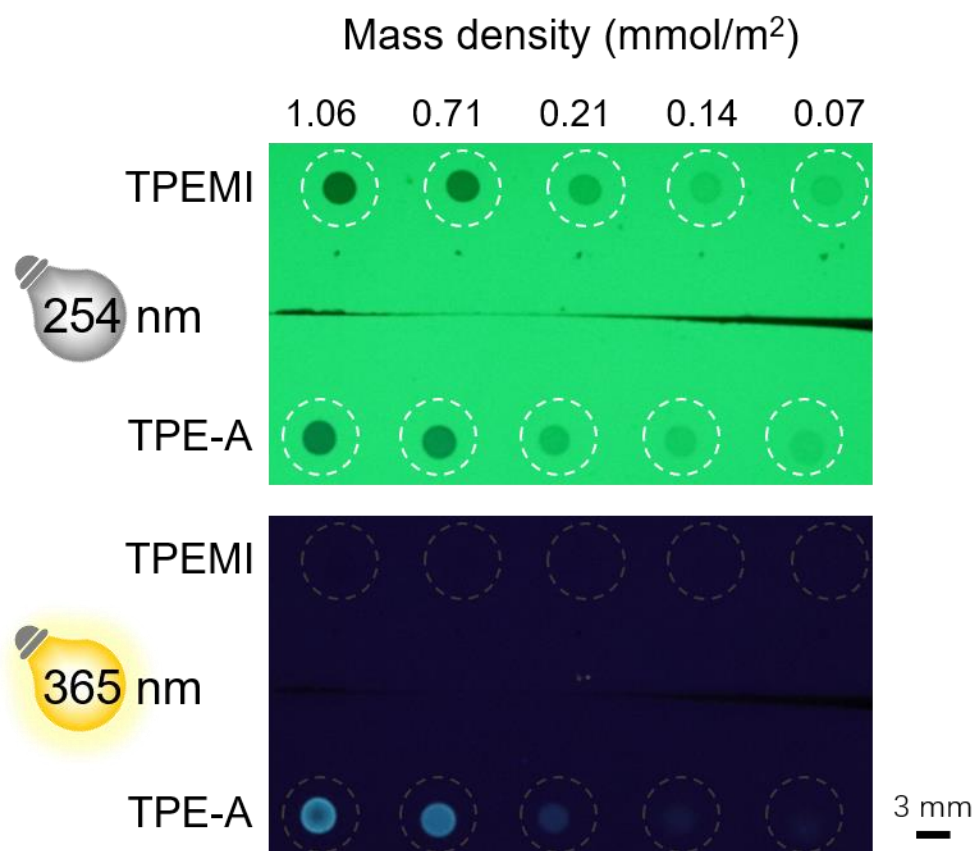


Figure S20. Photos of the sample dots containing gradient amount of TPEMI and TPE-A under UV light: 254 nm (top) and 365 nm (bottom).

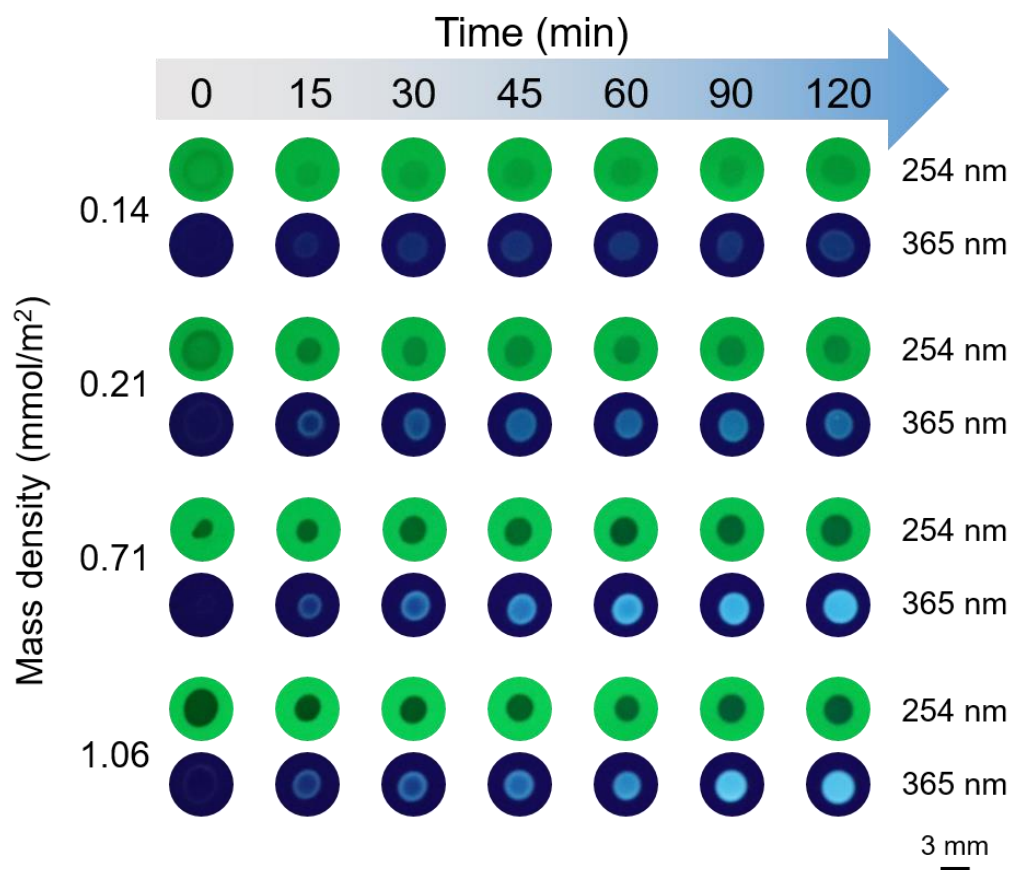


Figure S21. Photos of the sample dots containing gradient amount of TPEMI during heterogeneous DA reaction under UV light: 254 and 365 nm, respectively.

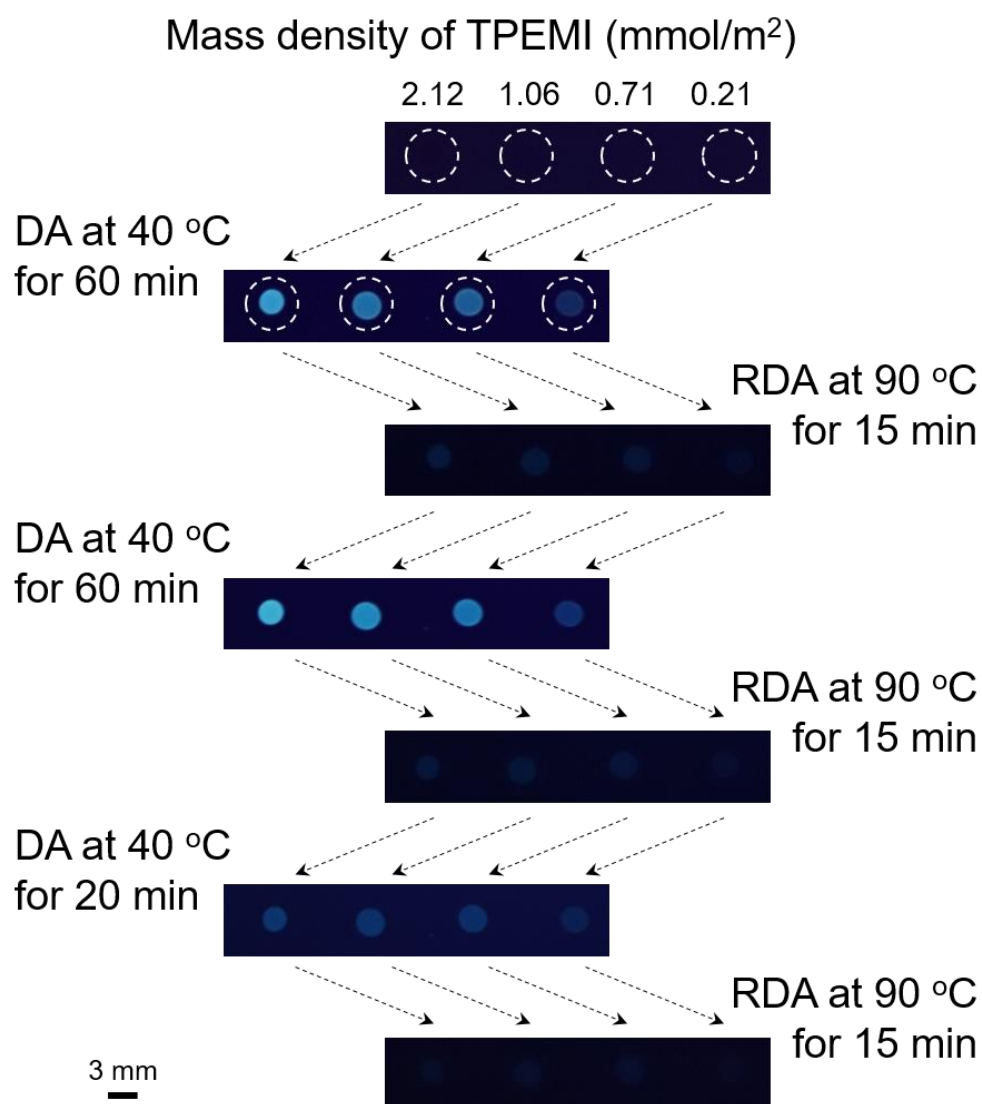


Figure S22. Reversible fluorescent “ON-OFF” switching from TPEMI in solid state on a silica plate.

DA reaction 1 mmol/L TPEMI in CH₃CN was obtained and dotted onto a silica plate with the glass capillary ($d = 3$ mm), then waited for several minutes to evaporate solvent. In a petri dish containing furfuryl alcohol, the silica plate was sealed for gradient time from 0 to 90 min. Then, thin layer chromatography (TLC) was used to study the relative content of TPEMI and TPE-A produced.

RDA reaction 1 mmol/L TPE-A in CH₃CN was obtained and dotted onto a silica plate with the glass capillary ($d = 3$ mm), then waited for several minutes to evaporate solvents. Under different selected temperatures (60 - 90 °C), the plate was heated on a heating stage for gradient time from 0 min to 3 h. Then, TLC was used to study the relative content of TPEMI and TPE-A remained.

As shown in Figure S23, the TLC results confirmed the production of TPE-A via heterogeneous DA reactions and TPEMI via solid state RDA reactions, respectively.

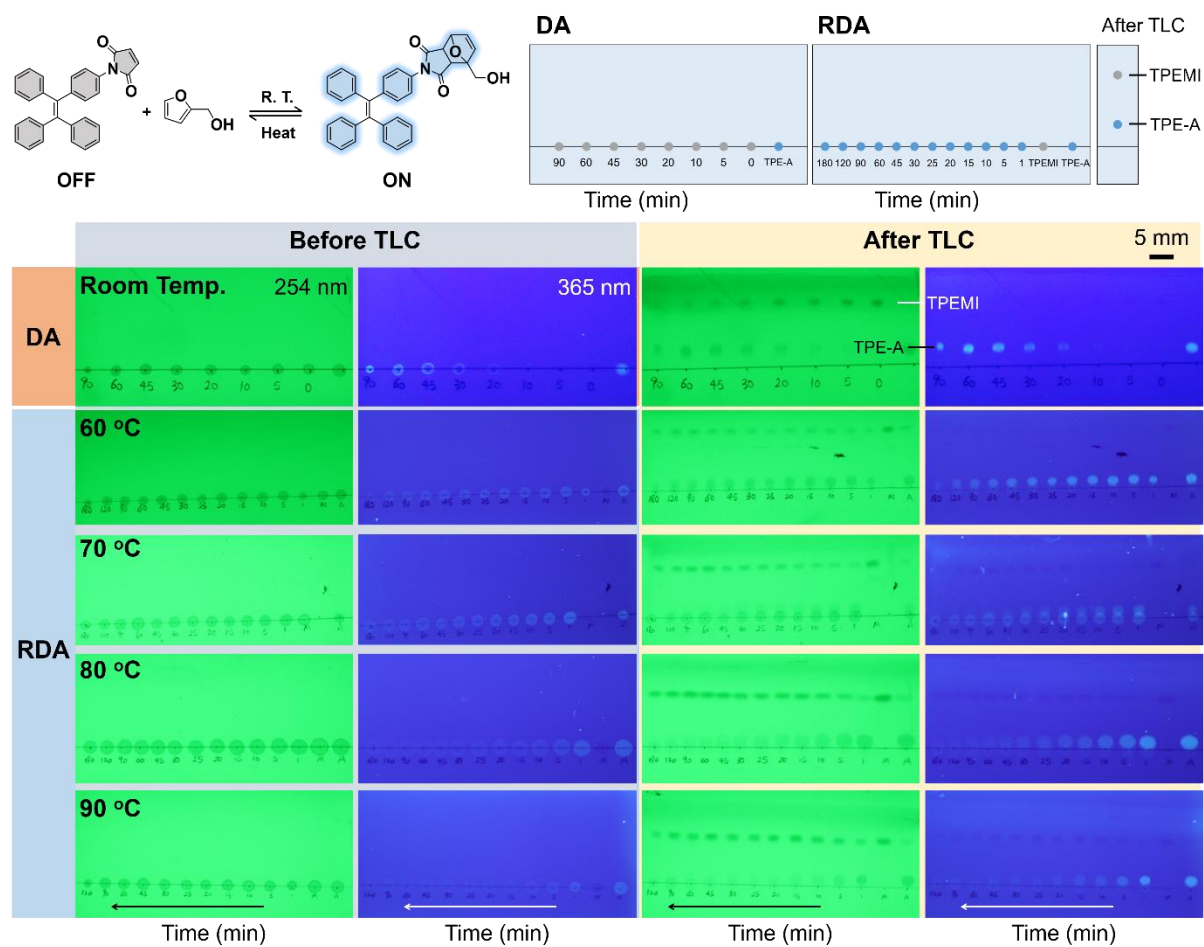


Figure S23. Photos of heterogeneous DA reactions and solid state RDA reactions at diverse temperatures on silica plates before and after TLC.